Structural, Electronic, and Vibrational Properties of $C_{60-n}N_n$ ($n = 1-12$)

Hitesh Sharma,[†,‡] Isha Garg,[†] Keya Dharamvir,[†] and V. K. Jindal*[,†]

Department of Physics, Center of Advanced Studies in Physics, Panjab University, Chandigarh 160014, and Department of Applied Sciences, Rayat and Bahra Institute of Engineering and Bio-Technology, Sahauran, Mohali, Punjab 140104

Received: March 4, 2009; Revised Manuscript Received: May 13, 2009

Ab initio investigation of structural, electronic and vibrational properties of nitrogen-doped fullerenes ($C_{60-n}N_n$, for $n = 1-12$) has been performed using numerical atomic orbital density functional theory. We have obtained the ground-state structures for $C_{60-n}N_n$ for $n = 1-12$, which show higher stability with a single nitrogen in a pentagon and two nonadjacent nitrogen atoms in a hexagon. Nitrogen doping leads to structural deformation, with the diameter showing variation from (7.14 − 0.24) to (7.14 + 0.10) Å. The average diameter of $C_{60-n}N_n$ shows a small decrease for $n \geq 5$, with a minimum value of 7.06 Å for $n = 12$. The change in the average diameter signifies the volume contraction, which is also maximum for $C_{48}N_{12}$. The binding energy per atom is found to decrease as a function of the number of N atoms. The HOMO−LUMO gap is found to decrease with an increase in substitutional nitrogen atoms; however, no systematic pattern could be observed. The Mulliken charge analysis performed on all optimized geometries shows a charge transfer of −0.3 to −0.45 (or 0.3−0.45 electrons) from nitrogen to carbon atoms, resulting in nitrogen atoms behaving as electrophilic sites. The harmonic vibrational frequency analysis shows the absence of any imaginary mode. The vibrational frequencies are found to decrease with an increase in the number of nitrogen atoms in $C_{60-n}N_n$. The results obtained are consistent with available theoretical and experimental results.

I. Introduction

In the recent past, extensive efforts have been made to understand the structural, electronic, and vibrational properties of pure fullerenes.[1] The properties of C_{60} have been altered by endohedral, substitutional, and exohedral doping.[1−4] In C_{60}, when one or more carbon atoms are replaced by nitrogen,[2] boron,[4] germanium[5] and silicon,[6−8] the structural and electronic properties show significant variation. The chemical, electrical, and magnetic properties of heterofullerenes need to be explored for a wide range of applications.[9,10] Nitrogen- and boron-doped fullerenes are of special importance as B-doped fullerenes behave as positive hole carriers and N-doped fullerenes act as electron carriers. N-doped fullerenes show enhanced chemical properties and exhibit variable electronic properties,[11,12] which make them potential candidates for applications in molecular electronics.

Ever since the discovery of N-doped fullerenes in 1995 by Hummelen and Wudl[3] in the dimeric form, it has been a subject of immense interest among researchers around the world. The experimental work on the nitrogen-doped heterofullerenes has provided significant progress with isolation of $C_{59}N$ in 1995,[13−15] $C_{48}N_{12}$ in 2001,[4] and $C_{57}N_3$ in 2008.[16] The formation of triazafullerene using the surface-catalyzed cyclodehydrogenation process[16] has even predicted the strong possibility of producing other members of the azafullerene family. Therefore, their systematic investigation deserves much needed attention.

Theoretically, there have been many isolated studies to predict the most stable structures of heterofullerenes ($C_{60-n}N_n$) and explain their structural and electronic properties. The structural and electronic properties of $C_{60-n}X_n$ (X = N and B) for $n = 1-2$ using the Huckel method[17] and the self-consistent field molecular orbital method[18] have been studied. Chen et al.[19−21] further studied heterofullerene structures for $n = 2$, 4, 6, and 8 using semiempiricial MNDO, AM1, PM3, and the Hartee−Fock method and further extended their studies to $C_{57}X_3$ and $C_{56}X_4$. Manaa[22] has studied the structural stabilities of $C_{48}N_{12}$. The chemical stability of oxygenated and hydrogenated $C_{48}N_{12}$ and $C_{58}N_{12}$ has been studied by Qiang et al.[23] using DFT-based calculations. The electronic properties of acceptor $C_{60-n}B_n$ and $C_{60-n}N_n$ donor pairs for $n = 1-12$ have been reported using first-principle calculations.[11,12] However, the geometries considered in these calculations, apart from $C_{48}N_{12}$, are arbitrary in nature and have been obtained by removing one nitrogen atom at a time from $C_{48}N_{12}$.[12] Because no vibrational and structural analysis has been performed on any of the structures, they may not correspond to global minima. The electronic properties of the heterofullernes depend upon the relative positions of substituted atoms in fullerenes. As the number of carbon atoms replaced by hetero atoms increases, a large number of theoretically possible isomers emerge. To our knowledge, the heterofullerenes with an odd number of nitrogen atoms (except for $C_{60}N$, $C_{57}N_3$, and $C_{50}N_{10}$) have not been reported in the literature. Therefore, a systematic search for the optimized ground-state structures of $C_{60-n}N_n$ for $n = 1-12$ is of immense importance.

Since, we have studied the structural properties of C_{60}[24,25] and C_{60} dimer[26,27] extensively using model potentials with good success; therefore, further studies with ab initio studies will improve our understanding of fullerene systems. In this paper, we report the results of our ab initio calculations of the structural and vibrational aspects for $C_{60-n}N_n$, $n = 1-12$. Since there is considerable inconsistency in predicting the electronic properties using various theoretical methods, we have extended our study to calculate the HUMO−LUMO gap and the electron density

* To whom correspondence should be addressed.
† Panjab University.
‡ Rayat and Bahra Institute of Engineering and Bio-Technology.

10.1021/jp901969z CCC: $40.75 © 2009 American Chemical Society
Published on Web 07/14/2009

TABLE 1: The Minimum Diameter, Maximum Diameter, C−N Bond Distance, and C−C Bond Distance in the Absence of Any Nitrogen in the Ring and in the Presence of One and Two Nitrogen Atoms in the Pentagon and Hexagon Rings of the Ground-State Structures and Isomers of $C_{60-n}N_n$ for $n = 0-12$ (all distances in Å)

$C_{60-n}N_n$	Dia_{Min}	Dia_{Max}	C−N (in Å)	C−C (with 2 N)	C−C (with 1 N)	C−C
0	7.14	7.14				1.40
						1.46
1	7.07	7.18	1.41		1.41	1.41−1.42
			1.43		1.46	1.45−1.46
2	7.10	7.23	1.40−1.43	1.39−1.41	1.40−1.43	1.42−1.44
			1.39−1.46	1.46−1.47	1.45−1.48	1.45−1.46
3	7.08	7.21	1.39−1.43	1.42−1.43	1.41−1.43	1.41−1.42
			1.41−1.44	1.43−1.44	1.43−1.46	1.45−1.46
4	7.08	7.24	1.43−1.44	1.42−1.43	1.41−1.42	1.41−1.42
			1.42−1.45	1.43−1.44	1.45−1.46	1.45−1.46
5	7.00	7.21	1.43	1.41−1.42	1.41−1.43	1.41−1.43
			1.43	1.42−1.43	1.43−1.46	1.44−1.46
6	6.95	7.18	1.43	1.40−1.43	1.41−1.43,	1.41−1.42,
			1.43	1.40−1.44	1.42−1.47	1.46−1.47
7	7.04	7.15	1.42−1.43	1.41−1.42	1.41−1.43	1.43−1.44
			1.43	1.43−1.46	1.42−1.46	1.44−1.46
8	7.04	7.19	1.42−1.43	1.43−1.44	1.41−1.44	1.43−1.44
			1.41−1.43	1.42−1.43	1.42−1.45	1.43−1.47
9	7.01	7.19	1.41−1.43	1.42−1.43	1.43−1.44	1.41−1.42
			1.41−1.43	1.41−1.42	1.41−1.43	1.44−1.45
10	6.97	7.20	1.42−1.43	1.42−1.44	1.43−1.45	1.42−1.43
			1.41−1.43	1.41−1.42	1.41−1.46	1.43−1.44
11	6.93	7.21	1.43	1.42−1.43	1.42−1.44	1.43
			1.42−1.43	1.42−1.43	1.41−1.46	1.43
12	6.90	7.22	1.42−1.43	1.43−1.45	1.42−1.44	1.43
			1.42−1.45	1.41−1.42	1.41−1.45	1.42

of states. Moreover, there are open questions about the charge distribution when compared with the neutral case and selection of the optimal conditions to enhance chemical reactivity. Mulliken charge analysis is performed to investigate the charge redistribution due to nitrogen substitution. The plan of the paper is that the Computational Details of the method are presented in section II, results and discussion are in section III, and Conclusions are in section IV.

II. Computational Details

We have used the Spanish Initiative for electronic simulation with thousands of atoms (SIESTA) computational code, which is based on the numerical atomic orbital density functional theory method.[28−30] The calculations are carried out using the generalized gradient approximation (GGA) that implements Becke's gradient exchange functional and Lee, Yang, and Parr's correlation functional (BLYP).[31−33] Core electrons are replaced by nonlocal, norm-conserving pseudopotentials factorized in the Kleinman−Bylander form,[34] whereas valence electrons are described using a linear combination of numerical pseudoatomic orbitals of the Sankey−Niklewski type[35] but generalized for multiple-ζ and polarization functions. In this work, we have used a split valence double-ζ polarized basis set (DZP). The cutoff is fixed by the "energy shift" parameter = 0.15 eV (the change in the eigen state of the free atom due to confinement). For self-consistent calculation of Hamiltonian matrix elements, the charge density is represented in a real space grid by a cutoff energy of 200 Ry. The cluster structures are obtained by minimization of the total energy using Hellmann−Feynman forces, including Pulay-like corrections. Structural optimizations were performed using the conjugate gradient algorithm until the residual forces in the optimization were smaller than 0.001 eV/Å. Periodic boundary conditions have been considered using a simple cubic shell of 20 Å that is large enough to avoid any significant spurious interactions with periodically repeated images.

We have performed test calculations on C_{60} and have found the C−C bond distances to be 1.40 and 1.46 Å, in agreement with experimental values of 1.40 and 1.46 Å for double and single bonds, respectively.[19] The ionization potential and electron affinity (6.9 and 2.70 eV) agrees well with their experimental values (7.5 ± 0.01[36] and 2.689 ± 0.008,[37] respectively).

III. Results

A. Structures and Energetics. We optimized the ground-state structures of $C_{60-n}N_n$ for $n = 1-12$ by finding the total energy by using DFT-based ab initio calculations. For each combination of nitrogen atoms, we have considered 15−20 different initial configurations (isomers) as starting geometries. The optimized geometries reported in the literature were also considered as initial configurations. All of the heterofullerenes $C_{60-n}N_n$ studied were found to exhibit many energetically close isomers involving multiple bonding. The optimized structural parameters such as C−C and C−N bond lengths of the optimized ground-state structures and energetically close isomers are presented in Table 1. The total energies, the binding energy, and the incremental binding energy of the $C_{60-n}N_n$ for $n = 1-12$ are tabulated in Table 2. The relative energies of all of the possible regioisomers of $C_{58}N_2$ with respect to the ground-state structure are tabulated in Tables 3 and 4. The Mullikan charges for all of the structures are listed in Tables 5 and 6. The optimized structure of C_{60} along with the numbering of atoms is shown in Figure 1. The optimized ground-state structures of heterofullerenes $C_{60-n}N_n$ are shown in Figures 2−6.

We started our calculations from the C_{60} molecule, which was optimized to the ground-state configuration until the atomic forces on each atom were reduced to 0.001 eV/Å. The structural properties of C_{60} such as the C═C and C−C bond lengths were found to be 1.40 and 1.46 Å, which are in excellent agreement with experimental values within two decimal places.[15] The mean diameter of C_{60} was found to be 7.14 Å, whereas the experimental value reported in the literature is 7.12 Å.[18] The

TABLE 2: Total Energy E_{total} (in eV) and Binding Energy (eV/atom) of the $C_{60-n}N_n$ for $n = 1-12$

$C_{60-n}N_n$	total energy (eV)	binding energy (eV/atom)	incremental binding energy
$C_{59}N$	−9337.14	7.55	
$C_{58}N_2$	−9456.85	7.53	0.02
$C_{57}N_3$	−9571.96	7.49	0.04
$C_{56}N_4$	−9687.17	7.46	0.03
$C_{55}N_5$	−9797.43	7.45	0.01
$C_{54}N_6$	−9912.66	7.44	0.01
$C_{53}N_7$	−10029.25	7.42	0.02
$C_{52}N_8$	−10147.39	7.40	0.02
$C_{51}N_9$	−10262.32	7.37	0.03
$C_{50}N_{10}$	−10372.17	7.35	0.02
$C_{49}N_{11}$	−10486.39	7.32	0.03
$C_{48}N_{12}$	−10600.68	7.28	0.04

binding energy was found to be 7.72 eV/atom, in agreement with the value quoted by Dresselhaus[1] but higher than that reported in the literature using DFT with the B3LYP hybrid functional.[11]

For $n = 1$, we substituted one carbon atom into the fullerene structure with the nitrogen atom at any vertex of the C_{60} molecule shown in Figure 1 and relaxed the structure until the desired convergence was reached. All of the positions were found to be nearly isoenergetic, and the energy difference between them is on the order of 0.01 eV.

Since the super cell considered is large enough, that is, 20 Å, we performed a total energy calculation with different periodic lattices of different sizes and found that there is negligible effect on the total energy of the system beyond 12 Å. Therefore, any effect of undesired interactions due to the periodic nature of the cell can be ruled out.

The resulting decrease in curvature around the nitrogen position changes the shape of the hexagon and pentagon rings. This distortion with respect to the C_{60} structure is expressed as the difference between the maximum and minimum diameter. The diameter varies from a maximum value of 7.18 Å to a minimum value of 7.08 Å in $C_{59}N$. However, the average diameter was found to be 7.14 Å, which is the same as that for C_{60}. The C═C and C−C bond distances were found to be 1.41 and 1.46 Å, respectively. The C−N distances varied from 1.41 to 1.43 Å. The C−N distance in the cyanide group was found to be 1.35 Å. The binding energy iwas found to be 7.55 eV/atom, which is of the same order as 6.88 eV/atom, predicted using the B3LYP hybrid density and 6-31G(d) basis set.[16] Thus, the binding energy difference between pure C_{60} and $C_{59}N$ is ∼0.19 eV.

For $n = 2$, we considered nitrogen substitution at different positions starting from two adjacent nitrogen atoms, alternate nitrogen positions in the hexagon ring and gradually increasing to the diagonally opposite position. The relative difference in energies of all possible 23 regioisomers is listed in Tables 3

TABLE 3: Relative Energies of Possible Regioisomers of $C_{58}N_2$[a]

Site indices of substituted pair (site 1 is always included)	Relative positions of the substituted N atoms	Relative Energy Difference (eV)
(1,10),(1,7)		0.00
(1,13), (1,14)	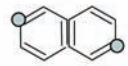	+0.02
(1,6),(1,42)	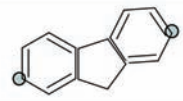	+0.03
(1,49)	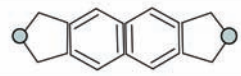	+0.10
(1,11), (1,21),(1,53), (1,39)	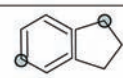	+0.13
(1,37)	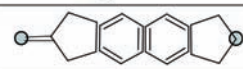	+0.14
(1,12), (1,36)	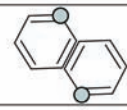	+0.16
(1,20), (1,32)	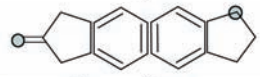	+0.19
(1,40),(1,29),(1,51),(1,60)	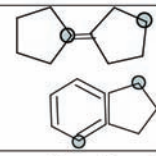 or	+0.20
(1,3), (1,56)	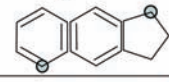	+0.21
(1,4), (1,35), (1,58),(1,52)	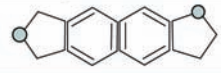	+0.21

[a] Energies are relative to that of the minimum-energy configuration, which has a total energy of −9456.86 eV.

TABLE 4: Relative Energies of Possible Regioisomers of $C_{58}N_2$[a]

Site indices of substituted pair (site 1 is always included)	Relative positions of the substituted N atoms	Relative Energy Difference (eV)
(1,30), (1,50),(1,55),(1,5)	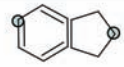	+0.27
(1,28),(1,59)	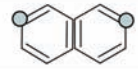	+0.27
(1,43), (1,23), (1,44), (1,38)	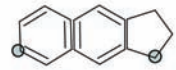	+0.29
(1,18),(1,31) (single bond)	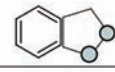	+0.30
(1,19) , (1,25)	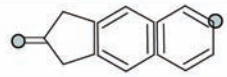	+0.31
(1,57),(1,15)	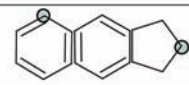	+0.32
(1,8), (1,9),(1,26),(1,41)	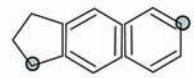	+0.36
(1,46), (1,24), (1,22), (1,47)		+0.39
(1,2), (1,54), (1,16), (1,45)	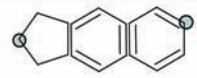	+0.41
(1,27),(1,17)	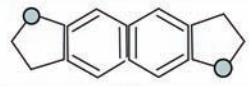	+0.41
(1,34),(1,48)		+0.47
(1,33) (double bond)	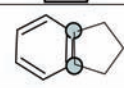	+0.70

[a] Energies are relative to that of the minimum-energy configuration, which has a total energy of −9456.86 eV.

TABLE 5: Net Charge on Nitrogen Atoms and Their NN Carbon Atoms from a Mulliken Charge Distribution of the $C_{60-n}N_n$ for $n = 1-8$[a]

$C_{60-n}N_n$	net charge (Q/e)	net charge (Q/e)	$C_{60-n}N_n$	net charge (Q/e)	net charge (Q/e)
$C_{59}N$	N(1) −0.431	C(18) +0.109	$C_{58}N_2$	N(1) −0.419	C(31) +0.099
		C(31) +0.100		N(7) −0.423	C(18) +0.264
		C(33) +0.135			C(22) +0.103
					C(53) +0.166
$C_{57}N_3$	N(1) −0.417	C(33) +0.246	$C_{56}N_4$	N(5) −0.393	C(46) +0.123
	N(5) −0.430	C(10) +0.161		N(10) −0.371	C(36) +0.141
	N(51) −0.428	C(39) +0.096		N(36) −0.392	C(1) +0.117
		C(43) +0.123		N(47) −0.372	C(48) +0.154
$C_{55}N_5$	N(9) −0.415	C(18) +0.119	$C_{54}N_6$	N(10) −0.391	C(24) +0.132
	N(28) −0.413	C(33) +0.131		N(22) −0.397	C(31) +0.127
	N(46) −0.458	C(41) +0.129		N(23) −0.417	C(39) +0.102
	N(50) −0.429	C(45) +0.103		N(29) −0.410	C(41) +0.116
	N(52) −0.428	C(59) +0.141		N(33) −0.391	C(42) +0.108
				N(59) −0.364	C(46) +0.240
$C_{53}N_7$	N(2) −0.399	C(30) +0.116	$C_{52}N_8$	N(2) −0.416	C(19) +0.129
	N(7) −0.411	C(32) +0.106		N(7) −0.384	C(20) +0.111
	N(37) −0.403	C(34) +0.139		N(27) −0.390	C(33) +0.264
	N(40) −0.376	C(20) +0.249		N(37) −0.381	C(22) +0.103
	N(42) −0.386	C(46) +0.102		N(40) −0.340	C(23) +0.118
	N(45) −0.383	C(49) +0.137		N(42) −0.375	C(24) +0.144
	N(51) −0.402	C(53) +0.112		N(45) −0.399	C(59) +0.136
				N(51) −0.380	C(30) +0.122

[a] The positive and negative signs represent charge gain and loss, respectively. The number mentioned in the bracket indicates the position of the atom with respect to the number scheme mentioned in Figure 1.

TABLE 6: Net Charge on Nitrogen Atoms and Their NN Carbon Atoms from a Mulliken Charge Distribution of the $C_{60-n}N_n$ for $n = 9-12$[a]

$C_{60-n}N_n$	net charge (Q/e)	net charge (Q/e)	$C_{60-n}N_n$	net charge (Q/e)	net charge (Q/e)
$C_{51}N_9$	N(2) −0.391	C(21) +0.103	$C_{50}N_{10}$	N(2) −0.401	C(19) +0.130
	N(7) −0.414	C(22) +0.114		N(7) −0.396	C(20) +0.109
	N(27) −0.365	C(23) +0.112		N(27) −0.355	C(59) +0.129
	N(29) −0.402	C(24) +0.147		N(29) −0.396	C(22) +0.111
	N(37) −0.381	C(26) +0.104		N(37) −0.385	C(23) +0.112
	N(40) −0.411	C(30) +0.127		N(1) −0.367	C(24) +0.149
	N(42) −0.417	C(32) +0.101		N(40) −0.414	C(30) +0.132
	N(45) −0.409	C(34) +0.139		N(42) −0.400	C(32) +0.103
	N(51) −0.380	C(35) +0.125		N(45) −0.409	C(34) +0.141
				N(51) −0.369	C(35) +0.122
$C_{49}N_{11}$	N(2) −0.401	C(39) +0.096	$C_{48}N_{12}$	N(2) −0.398	C(13) +0.124
	N(7) −0.402	C(22) +0.105		N(7) −0.389	C(34) +0.151
	N(27) −0.340	C(23) +0.220		N(27) −0.338	C(8) +0.257
	N(29) −0.412	C(24) +0.149		N(29) −0.422	C(17) +0.107
	N(37) −0.377	C(30) +0.127		N(37) −0.389	C(19) +0.123
	N(39) −0.358	C(32) +0.124		N(39) −0.349	C(20) +0.115
	N(40) −0.399	C(34) +0.139		N(40) −0.382	C(21) +0.109
	N(41) −0.376	C(8) +0.151		N(41) −0.392	C(22) +0.100
	N(42) −0.446	C(38) +0.121		N(42) −0.458	C(23) +0.219
	N(45) −0.394	C(46) +0.128		N(45) −0.408	C(24) +0.139
	N(51) −0.364	C(48) +0.144		N(51) −0.370	C(58) +0.145
				N(54) −0.351	C(30) +0.121

[a] The positive and negative signs represent charge gain and loss respectively.

and 4. We find that the most stable structure is the one with nitrogen at the (1,7) position (isoenergetic with (1,10)). This corresponds to nitrogen atoms at opposite vertices of a hexagon ring. If the N−N separation is decreased to the (1,18) and (1,33) positions, that is, nitrogen atoms at the ends of a double bond or a single bond, the structure becomes unstable by 0.70 and 0.30 eV, respectively. The next preferable positions for nitrogen atoms are (1,13) (isoenergetic to (1,14)) and (1,6) (isoenergetic to (1,42)), which are higher in energy by 0.02 and 0.03 eV, respectively. Upon placing nitrogen atoms at opposite ends of a diameter of the spherical C_{60} shell, that is, (1,37), the structure is less stable by 0.14 eV with respect to the lowest-energy structure. Chen et al.[19] suggested the (1,46) structure as the most stable one, but we found this configuration to be much higher in energy, by 0.39 eV. There are a large number of structures which are higher by ∼0.16−0.21 eV from the ground-state structure (see Table 3). There seems to be no correlation between the structures which have larger energy differences with respect to the lowest-energy structure.

The extent of distortion is shown by maximum and minimum diameters, which are found to be 7.23 and 7.10 Å, respectively. The average diameter is still 7.14 Å. The distortions and bond lengths for a few of the isomers are shown in Figure 2. The C−N bond distances are found to be 1.40−1.43 and 1.39−1.46 Å at the hexagon−hexagon (6,6) and hexagon−pentagon (6,5) interfaces, respectively. However, the C−N distance predicted using the molecular method by Noriyuki Kurita et al.[18] is in the range of 1.48−1.52 Å. The C═C and C−C bond distances in other neighboring rings with no nitrogen atoms also show increases of 1.42−1.44 and 1.45−1.46 Å. The binding energy shows a slight decrease to a value of 7.53 eV/atom from 7.72 eV/atom for C_{60}. The other theoretical studies had predicted the binding energies for $C_{58}N_2$ to be 5.90[18] and 6.82 eV.[16]

$C_{57}N_3$, that is, triazafullerene, has been experimentally produced and isolated successfully very recently.[16] We found that the most stable structure is the one with nitrogen at the (1,5,51) positions. We have considered many isomers ranging from all nitrogen in one ring at different positions to increasing the internitrogen atom distance as shown in Figure 3. We found that the structures shown are one or the other arrangement of $C_{58}N_2$ with one more substitution. The configuration (24,34,39) shown in Figure 3b and reported in ref 16 is found to be less stable by a small energy difference of 0.03 eV. However, if the PBE exchange interactions are considered, the (24,34,39) configuration is found to be more stable by 0.3 eV. The C−N, C−C, and C═C distances for four isomers with lowest energies in succession are shown in Figure 3. The diameter of $C_{57}N_3$ varies from a maximum value of 7.21 Å to a minimum of 7.08 Å, with an average value of 7.14 Å. The binding energy is found to be 7.49 eV/atom, which differs by 0.23 eV from that of the pure C_{60} molecule.

Figure 4 shows the optimized structures from $n = 4$ to 7. For $n = 4$, the nitrogen atoms at (5,10,36,47) yield the most stable structure. The obtained ground-state structure of $C_{56}N_4$ agrees with the structure proposed using the semiempirical method by Chen et al.,[19] and it shows the diameter variation from a maximum of 7.24 Å to a minimum of 7.08 Å, with an average diameter of 7.14 Å. The C−N and C−C bond lengths are shown in Figure 4. The binding energy is found to be 7.46 eV/atom, which is higher than that obtained from calculations using ab initio methods with the B3LYP functional.[11] The binding energy difference of $C_{56}N_4$ and pure C_{60} comes out to be 0.26 eV. Interestingly, we find that if we substitute four nitrogens in one pentagon ring, the structure shows opening of the heterofullerene $C_{56}N_4$ by breaking of the N−N bond (Figure 7).

For $n = 5$, nitrogen atoms substituted at the (9,28,46,50,52) positions in C_{60} give rise to the stable structure. From the isomers considered, it is found that if we replace all five carbon atoms by nitrogen atoms in a pentagon ring, the $C_{55}N_5$ structure opens up, that is, breaking of the cage structure takes place (see Figure 7), and is unstable by 3.56 eV. The $C_{55}N_5$ structure shows significant distortion with respect to C_{60}; the diameter varies from a maximum of 7.21 Å to a minimum of 7.00 Å. However, the average diameter shows no variation up to the second decimal with respect to to the average diameter, that is, 7.14 Å in C_{60}. The C−N and C−C bond distances are shown in Figure

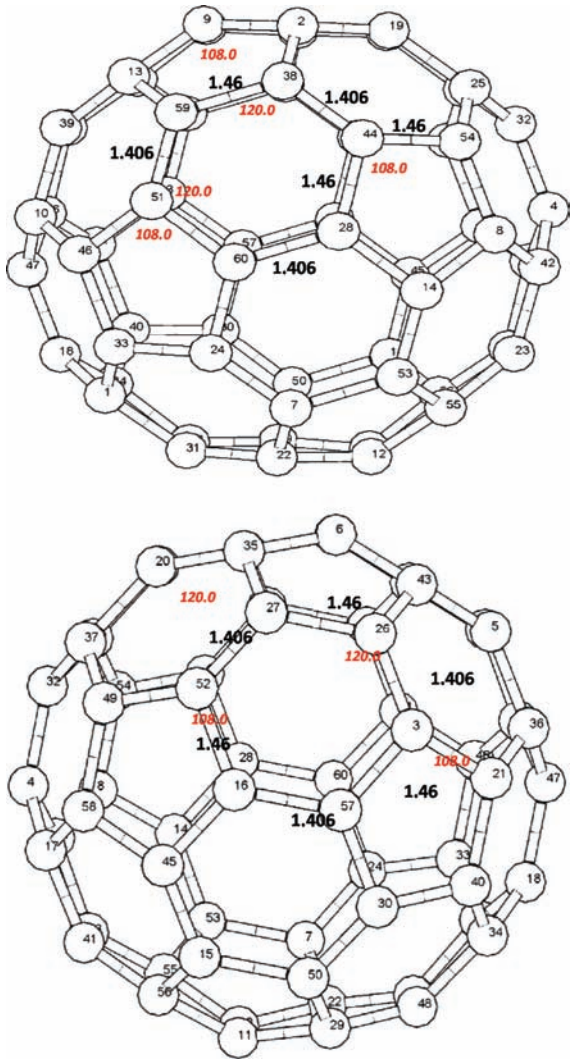

Figure 1. Optimized geometry of C_{60} and numbering of the carbon atoms which are used to indicate the doping sites of the nitrogen atoms. The calculated C−C and C═C bond distances and bond angles are expressed in Angstroms and degrees, respectively.

4. The binding energy is found to be 7.45 eV/atom, with a binding energy difference of 0.27 eV from pure C_{60}.

For $n = 6$, the structure with nitrogen atoms at (10,22,23,29,33,59) in C_{60} is found to be the most stable. The structure with nitrogen at (10,19,22,32,44,59) is found to be nearly isoenergetic, with a very small energy difference of 0.001 eV. However, using the PM3 method, Chen et al.[19] predicted the second structure mentioned above to be more stable than the first one. The opening up of the $C_{54}N_6$ structure when six nitrogen are substituted in one hexagon ring is shown (Figure 7). The $C_{54}N_6$ structure shows significant distortion with respect to C_{60}; the diameter varies from a maximum of 7.18 Å to a minimum of 6.95 Å. However, the average diameter shows a decrease to 7.09 Å with respect to C_{60}, indicating a decrease in the average volume, that is, contraction of the $C_{54}N_6$ structure. The bond distances are shown in Figure 4. The binding energy is found to be 7.44 eV/atom with binding energy difference of 0.28 eV from that of pure C_{60}.

The ground-state structure of the $C_{53}N_7$ has not been reported experimentally nor theoretically in the literature. Nitrogen atoms placed at the (2,7,37,40,42,45,51) positions in C_{60} yield the most stable configuration compared to the other isomers optimized. The $C_{53}N_7$ structure shows nitrogen atoms distributed more or less evenly over the buckyball surface (Figure 4). The $C_{53}N_7$ structure shows significant distortion with respect to C_{60}; the diameter varies from a maximum of 7.15 Å to a minimum of 7.04 Å. The average diameter is found to be 7.10 Å, indicating a decrease of 0.04 Å with respect to pure C_{60}. The binding

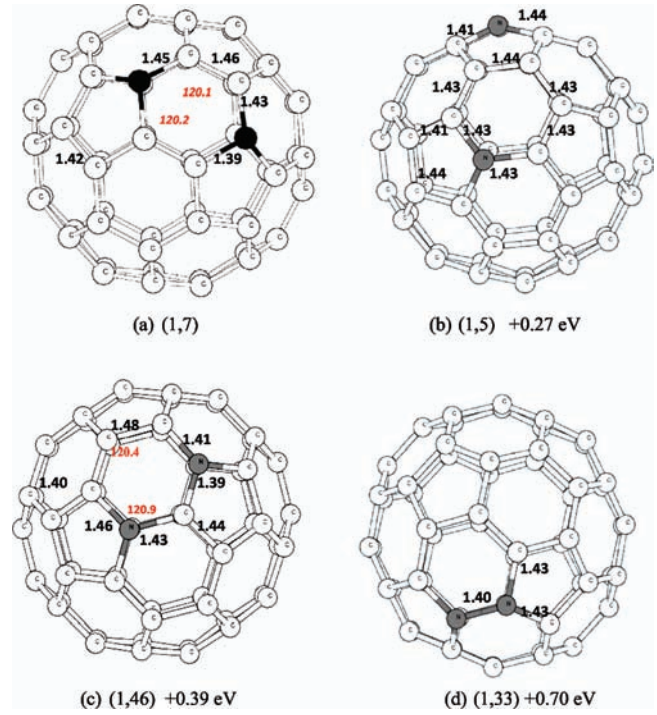

Figure 2. Optimized ground-state structure of $C_{58}N_2$ and its isomers with the difference in their energies with respect to the ground-state structure. The dark and white spheres denote nitrogen and carbon atoms, respectively. The calculated C−C, C═C, and C−N bond distances and bond angles are expressed in Angstroms and degrees, respectively.

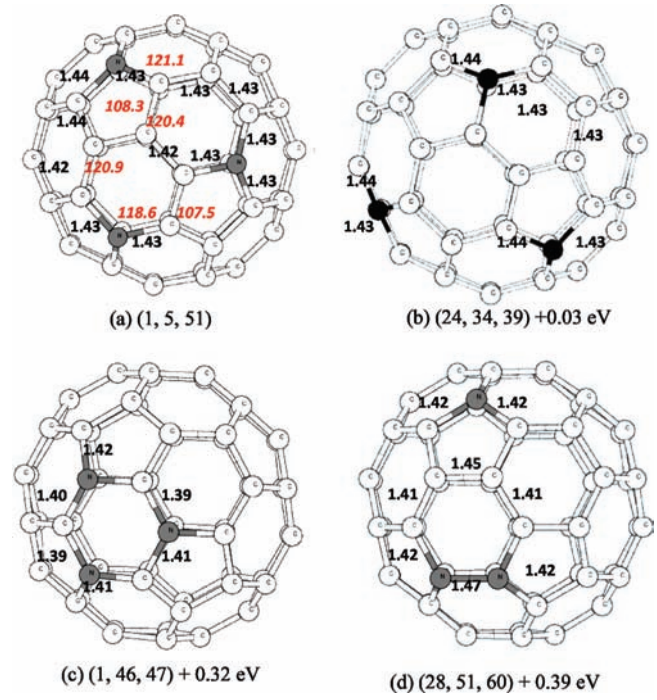

Figure 3. Optimized ground-state structure of $C_{57}N_3$ and its isomers with the difference in their energies with respect to the ground-state structure. The dark and white spheres denote nitrogen and carbon atoms, respectively. The C−C, C═C, and C−N bond distances are expressed in Angstroms, and bond angles are expressed in degrees.

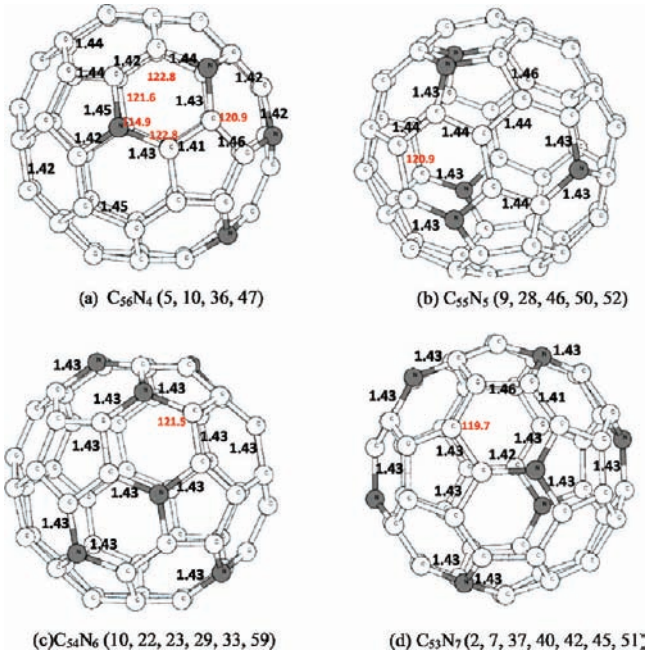

Figure 4. Optimized ground-state structure of $C_{60-n}N_n$ for $n = 4-7$. The dark and white spheres denote nitrogen and carbon atoms, respectively. The calculated C−C, C═C, and C−N bond distances and bond angles are expressed in Angstroms and degrees, respectively.

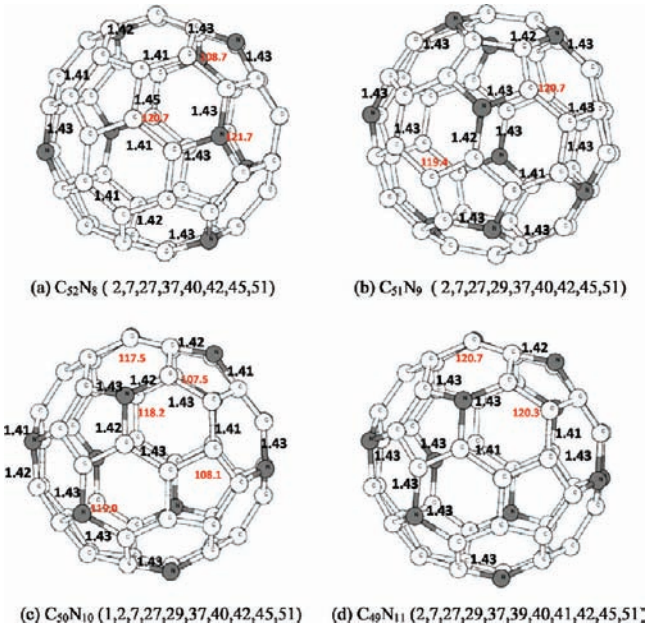

Figure 5. Optimized ground-state structure of $C_{60-n}N_n$ for $n = 8-11$. The dark and white spheres denote nitrogen and carbon atoms, respectively. The calculated C−C, C═C, and C−N bond distances and bond angles are expressed in Angstroms and degrees, respectively.

energy is found to be 7.42 eV/atom, having a binding energy difference of 0.30 eV when compared to that of pure C_{60}.

For $n = 8$, when nitrogen atoms are placed at the (2,7,27,37,40,42,45,51) positions in C_{60}, it results in the most stable structure (Figure 4). Once again, the ground-state structure has nitrogen atoms evenly distributed over the surface. The cage opening is also observed at two sites in the C_{60} molecule where four nitrogen atoms per ring are substituted to form $C_{52}N_8$ (Figure 7). The $C_{52}N_8$ structure shows significant distortion with respect to C_{60}, the diameter ranging from a maximum of 7.19 Å to a minimum of 7.04 Å. The average diameter is found to be 7.09 Å. The binding energy is found to be 7.40 eV/atom, with a binding energy difference of 0.32 eV compared to that of pure C_{60}. This structure is virtually the same as that of the minimum energy-structure of $C_{53}N_7$ (see site numbers within brackets), except for the additional nitrogen atom occupying site 27. It is also observed that the lowest-energy structures for $n = 6$, 7, and 8 have no more than one nitrogen atom per pentagon ring. For a hexagon ring, there may be more than one nitrogen atom but not at adjacent sites.

To obtain the lowest-energy structures for $n = 9$, 10, 11, and 12, one just has to add 1, 2, 3, and 4 nitrogen atoms at positions (29), (1,29), (29,39,41), and (29,39,41,44) to the $n = 8$ structure shown in Figure 5, that is, nitrogen at (2,7,27,37,40,42,45,51). Out of these, only the $C_{48}N_{12}$ structure (Figure 6a) contains a pentagon with two nitrogen atoms. In all of these structures, the maximum diameter is around 7.20 Å, whereas the minimum diameter steadily decreases from 7.01 to 6.90 Å, showing an increasing amount of local distortion at nitrogen sites. The average radius and the cohesive energy also increase steadily, as shown in Figures 8 and 9, respectively. It is rather surprising that the $C_{48}N_{12}$ structure with the lowest energy has two nitrogen atoms in a pentagon. Therefore, we looked carefully at the structures with one nitrogen per pentagon and found Figure 6b as the stable structure, with an energy a bit higher than the minimum-energy structure. Moreover, the open-cage structures for $n = 10$ and 12 are shown in Figure 7. For the sake of brevity, we have not shown all of the isomers for $n \geq 4$.

From the structural analysis of all of the ground-state structures of $C_{60-n}N_n$ for $n = 1-12$, it may be concluded that N atoms have preferential sites for its substitutions in fullerenes such that it minimizes the bond strain energy, which is considerably high in pure C_{60}. We observed that one nitrogen atom per pentagon ring is found to be more stable in all heterofullerenes than their isomers. Therefore, it may be concluded that weak N−N bonds are unstable and, therefore, should be avoided. However, if we substitute two nitrogen atoms in a ring, the stability decreases marginally. Further, if we increase the number of nitrogen atoms to more than two in the ring, then the structure is found to be least stable energetically. If we substitute all of the C atoms with heteroatoms in a ring of the cage structure, it becomes unstable. For $n \geq 4$, if all of the four nitrogen atoms or more are substituted in one pentagon or hexagon ring, the heterofullerene structure opens up by breaking of the N−N bond, that is, breaking of the cage structure. Therefore, in heterofullerenes, nitrogen atoms follow some rules, which are (a) pentagons may not have more than one nitrogen atom; (b) hexagons may have more than one nitrogen atom, but they should not be adjacent; and (c) the preferred positions for nitrogen atoms are at third or fourth neighbor sites.

Each heterofullerene structure shows regioisomerism, showing a large number of structures with a very small difference in energy. Nitrogen-induced modification can be attributed to the changes in the bond lengths and bond angles due to the formation of C−N bonds instead of C−C bonds and additionally to the capability of nitrogen to accommodate in different local atomic arrangements. The average C═C and C−C bond length range shows gradual shortening with an increase in the number of nitrogen atoms from 1.40 and 1.46 Å in the pure fullerene structure to 1.42 and 1.43 Å in $C_{48}N_{12}$. This may be attributed to the redistribution of the electron charge density. The C−N bond distances are found to vary from ∼1.40 to 1.44 Å in all of the structures.

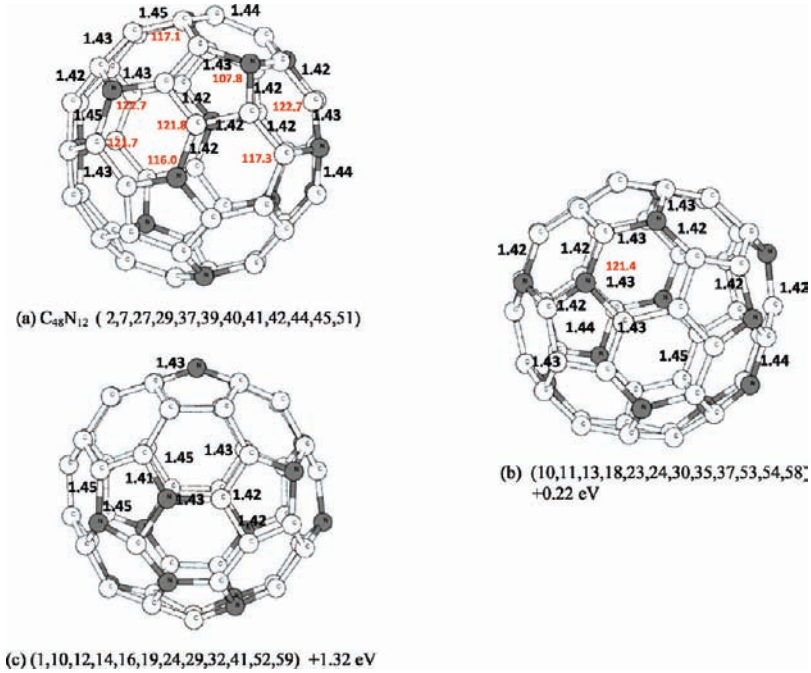

Figure 6. Optimized ground-state structure of $C_{48}N_{12}$ and its isomers with the difference in their energies with respect to the ground-state structure. The dark and white spheres denote nitrogen and carbon atoms, respectively. The calculated C−C, C═C, and C−N bond distances and bond angles are expressed in Angstroms and degrees, respectively.

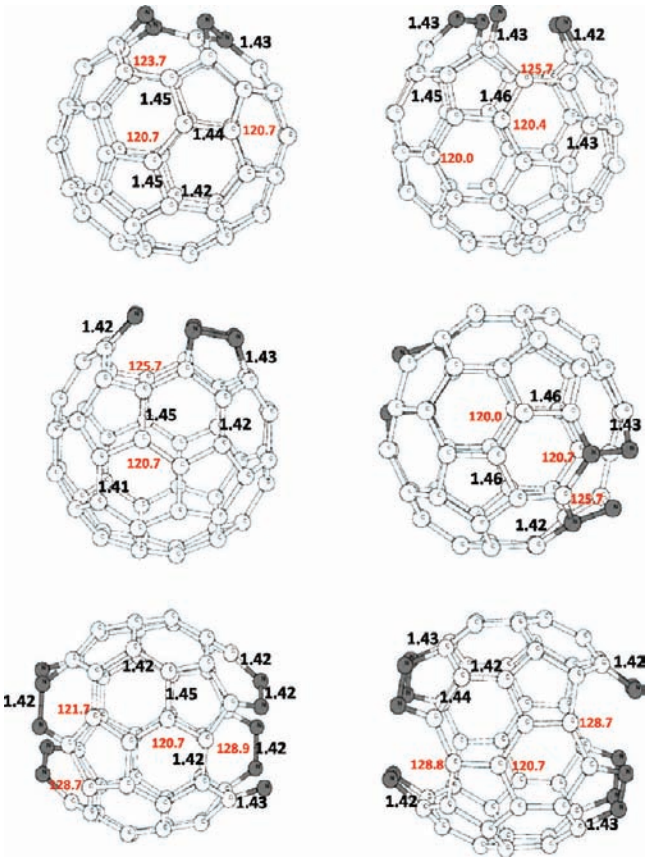

Figure 7. The optimized open-cage isomer structures of $C_{60-n}N_n$ for $n = 4$, 5, 6, 8, 10, and 12. The dark and white spheres denote nitrogen and carbon atoms, respectively. The C−C, C═C, and C−N bond distances are expressed in Angstroms, and bond angles are expressed in degrees.

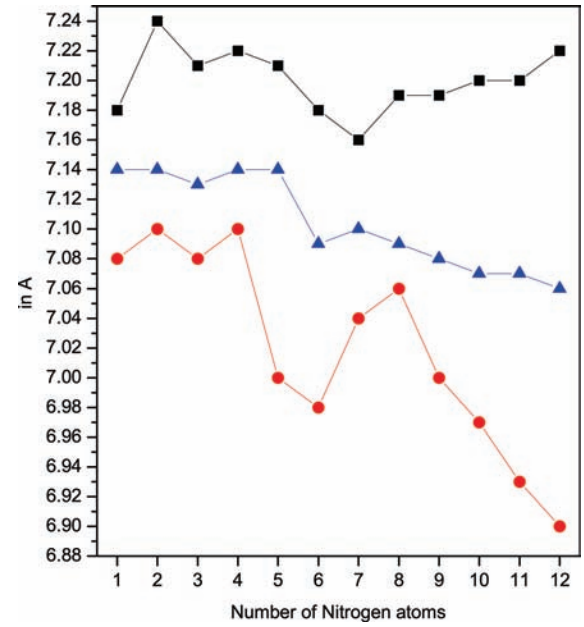

Figure 8. Maximum (square), average (triangle), and minimum diameter (circle) in Angstroms of $C_{60-n}N_n$ for $n = 1-12$ as a function of number of nitrogen atom.

The structural distortion measured in terms of the difference of the maximum and minimum diameters suggests that distortion increases with the number of nitrogen dopants, with a maximum for $n = 12$. The minimum diameter shows a maximum value for $C_{58}N_2$ and a minimum value for $C_{48}N_{12}$. The maximum diameter shows a minimum value for $C_{53}N_7$ and a maximum for $C_{56}N_4$, as shown in Figure 6. The difference between the maximum diameter and the minimum diameter gradually increases, with a maximum value for $n = 12$. The average diameter of the heterofullerene shows no significant change until $n = 5$ and decreases rapidly from $n = 5$ to 6. However, for $n \geq 6$, the heterofullerene structures start showing a gradual decrease of the average diameter, with a minimum value of 7.06 Å for $C_{48}N_{12}$.

The binding energy decreases gradually with increasing nitrogen atoms in heterofullerene $C_{60-n}N_n$, as shown in Table

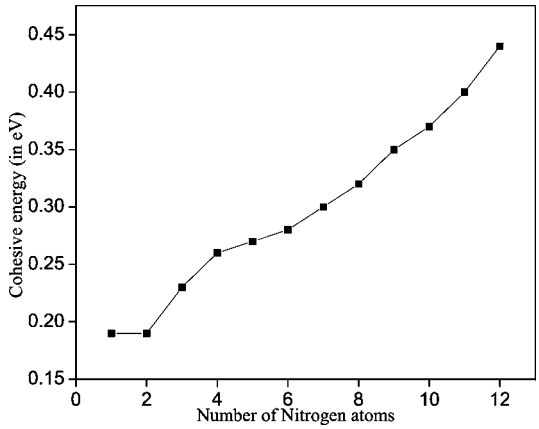

Figure 9. Variation of cohesive energy as a function of the number of nitrogen atoms, $n = 1-12$.

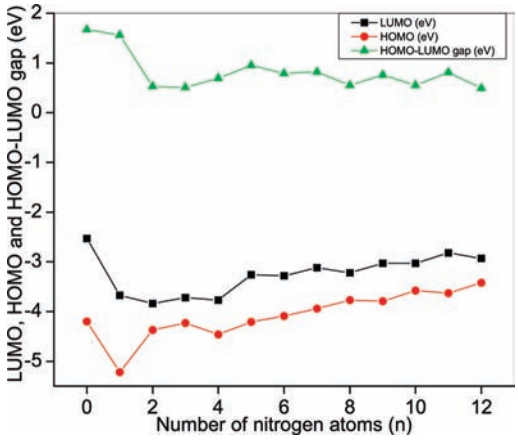

Figure 10. Variation of the LUMO, HOMO, and HOMO−LUMO gap in eV as a function of the number of nitrogen atoms, $n = 0-12$.

2. The value of the binding energy obtained is found to be slightly higher than that obtained using the B3LYP hybrid functional;[11] however, the incremental binding energy is found to be in good agreement. The binding energy difference between pure C_{60} and $C_{60-n}N_n$ is gradually increasing.

B. Electronic Properties. The nitrogen doping in C_{60} leads to distortion in the structures as discussed in the earlier section. As a result of doping, the icosahedral (I_h) symmetry of the C_{60} molecule is disturbed. The distortion in the symmetry and addition of nitrogen are expected to change the electronic distribution and hence electronic properties. One of the significant changes is in the energy difference of the highest occupied molecular orbital (HOMO) and the lowest unoccupied molecular orbital (LUMO). The variation of the LUMO energy level, the HOMO energy level, and the HOMO−LUMO gap of $C_{60-n}N_n$ for $n = 1-12$ is shown in Figure 10. We observed that the HOMO−LUMO gap shows a sharp decline from $n = 1$ to 2 and a small variation thereafter. In general, an odd number of nitrogen atoms shows a slightly larger band gap as compared to that of an even number of nitrogen atoms. It seems that this kind of pattern is due to the redistribution of electrons in energy levels as a result of addition of nitrogen atoms in the C_{60} molecule.

Moreover, the HOMO level continues to increase, which can be attributed to the fact that the degeneracy of the LUMO is lifted due to the doping of nitrogen atoms. In Figure 11, the Kohn−Sham energy eigen values of the $C_{60-n}N_n$ molecules for $n = 1$, 3, 7, and 12 are shown. The electronic polarization due

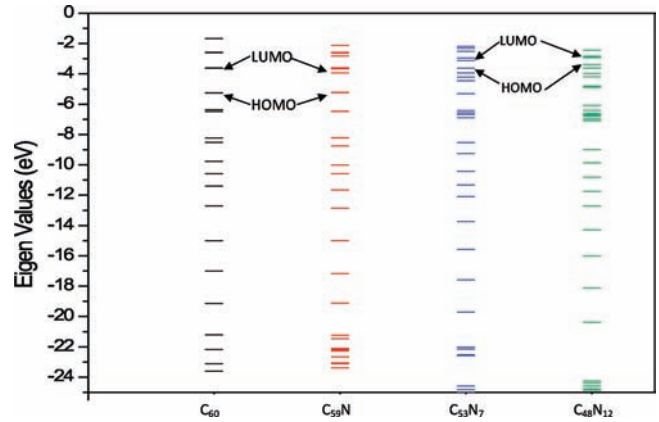

Figure 11. Kohn−Sham energy Eigen values of C_{60}, $C_{59}N$, $C_{57}N_3$, and $C_{48}N_{12}$. Only the lowest-energy eigen values and eigen values near the Fermi level are shown, indicating the HOMO−LUMO gap.

to nitrogen in the $C_{60-n}N_n$ is studied using Mulliken charge analysis on the site charge of atoms. The net charge on nearest neighbors around the nitrogen atom is tabulated in Tables 5 and 6. The positive and negative signs indicate charge gain and loss, respectively. We have also calculated the electron affinities and ionization potentials of the structures which have been experimentally observed.

The HOMO−LUMO gap of C_{60} is found to be 1.67 eV, which is less than 1.80 eV reported using B3LYP.[38] The ionization potential and electron affinity are found to be 6.9 and 2.69 eV, which are in fair agreement with experimental values of 7.5 ± 0.1[36] and 2.70 ± 0.008 eV,[37] respectively. The HOMO level is at −4.20 eV, and the LUMO, which shows three-fold degeneracy, is at a value of −2.53 eV. The Mulliken charge analysis of C_{60} shows a net charge of $Q_m = 0$ at all carbon sites showing total isotropy.

In $C_{59}N$, one carbon atom is replaced by nitrogen and has one extra electron. The three-fold LUMO degeneracy (t_{1u}) of C_{60} is lifted, and one of these levels is occupied by the extra electron. The charge loss and gain have been denoted by negative and positive signs, respectively. The Mulliken charge analysis shows a net charge in Q/e ($e = 1.6 \times 10^{-19}$ C) of −0.431 on the nitrogen atom and +0.100, +0.109, and +0.135 on the nearest-neighbor (NN) carbon atoms. In other words, nitrogen is donating 0.431 electrons to the surrounding carbon atoms. A similar pattern in charge transfer has been observed by Rui Xie et al.,[11] and they predicted the HOMO−LUMO gap to be 1.09 eV. The calculated values of the electron affinity and ionization potential are found to be 3.88 and 3.95 eV, respectively.

In $C_{58}N_2$, the HOMO−LUMO gap is found to decrease to 0.53 eV, which is of the same order as 0.01−0.57 eV predicted using the Huckel method,[17] 0.23−0.28 eV using the molecular orbital method,[13] 0.73 eV using time-dependent density functional theory,[12] and 0.93 eV using DFT with B3LYP-6-31(d).[11] The calculated values of the electron affinity and ionization potential are found to be 3.83 and 3.88 eV, respectively. For $C_{57}N_3$, the electron affinity and ionization potential are found to be 3.76 and 4.17 eV, respectively. Also, the HOMO−LUMO gap for all of the structures is found to be of the same order as that reported using DFT with B3LYP.[11] Now in $C_{53}N_7$, due to doping of seven nitrogen atoms, the LUMO with t_{1u} symmetry splits into three nondegenerate levels and so does the second LUMO (which has t_{1g}) symmetry in C_{60}. In $C_{48}N_{12}$, all of the energy levels, that is, the first and second LUMO, are filled up. The calculated values of the electron affinity and ionization potential are found to be 3.34 and 2.79 eV, respectively.

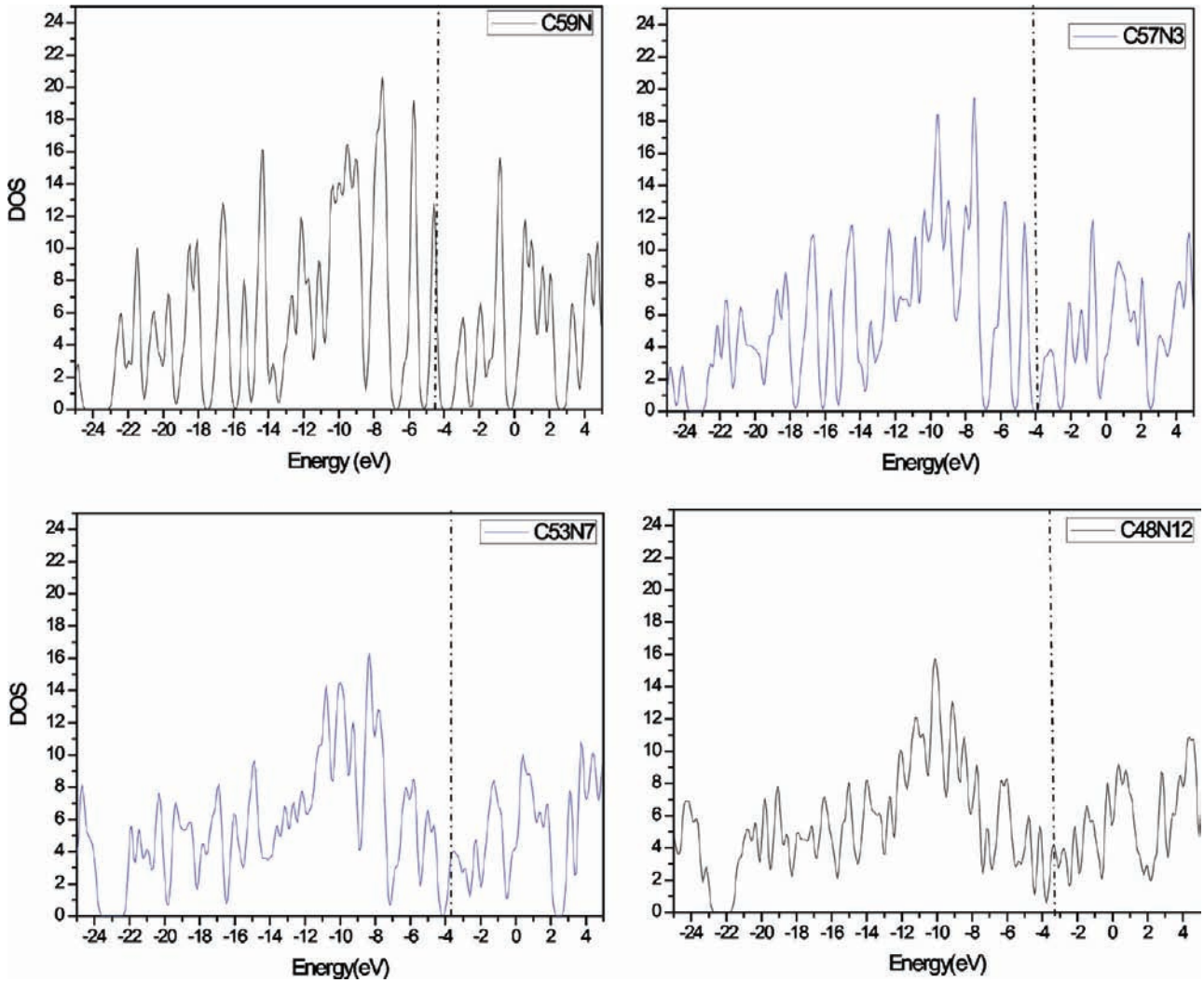

Figure 12. Electronic density of states (DOS) of $C_{60-n}N_n$ for $n = 1$, 3, 7, and 12. The dotted vertical line indicates the Fermi level in Kohn−Sham eigen values.

From the whole analysis done above, we observe that due to the introduction of heteroatoms in the fullerene cage structure, there is an unbalanced charge distribution in heterofullerene structures. Since nitrogen carries positive charge after loosing electrons to carbon atoms and negative charge is carried by their adjacent carbon atoms after gaining charge, it makes them preferential sites for electrophilic and nucleophilic attack, respectively. Also, the net charge transfer in structures up to $n = 6$ show one-third of all of the carbon atoms with negative charge transfer on the order of 0.004, whereas for $n \geq 7$, the number of carbon atoms with net negative charge transfer continues to decrease. This may be attributed to the even distribution of nitrogen atoms in azafullerenes.

The doped fullerene structures have higher electron affinity and a lower ionization potential as compared to those of pure C_{60}, which is consistent with the results obtained by Chen et al.[19] using MNDO and AM1 methods. The electronic density of states (DOS) of $C_{60-n}N_n$ for $n = 1$, 3, 7, and 12 is shown in Figure 12. The nitrogen doping in $C_{60-n}N_n$ shows significant change in the DOS and in the innermost energy states. The innermost states are found to vary from −23.60 eV for C_{60} to −25.54 eV for $C_{59}N$, −25.67 eV for $C_{57}N_3$, and −26.89 eV for $C_{48}N_{12}$.

C. Vibrational Properties. The vibrational analysis of C_{60} in harmonic approximation has been performed. The infrared (IR) vibrational frequency modes are found to be 526.2, 575.4, 1174.3, and 1460 cm^{-1}, which agree well with 527, 577, 1183, and 1428 cm^{-1}. The Raman-active frequency modes are found to be 489.3 and 1460 cm^{-1} with A_g symmetry, which are in agreement with experimental values of 496 and 1470 cm^{-1}. The Raman-active modes with H_g symmetry are found to be 253.2, 460.4, 717.5, 1451, and 1575.1 cm^{-1}, in agreement with experimental values of 273, 437, 710, 1428, and 1575 cm^{-1}, respectively.

The vibrational frequencies of all heterofullerenes have been calculated in the harmonic approximation. The five lowest and highest frequencies are shown in Figures 13 and 14, respectively. An isolated study of vibrational properties of $C_{48}N_{12}$ by Xie et al.[41] using the B3LYP hybrid functional has been reported. All of the frequency modes show a gradual decrease in magnitude with the number of nitrogen dopants. The number of degenerate frequency modes changes significantly with the distortion to 58 IR-active and 58 Raman-active modes in the $C_{48}N_{12}$ structure from 4 and 10 modes in pure C_{60}. The frequency range shows a shift of 15−78 cm^{-1} from the pure C_{60} structure. Such behavior may be attributed to an increase in the mass of heterofullerenes with respect to C_{60}. The lowest-frequency decreases with an increase in the number of nitrogens doped, from 248.4 in C_{60} to 226.4 cm^{-1} in $C_{48}N_{12}$, whereas the highest modes do not show any systematic pattern. The zero-point

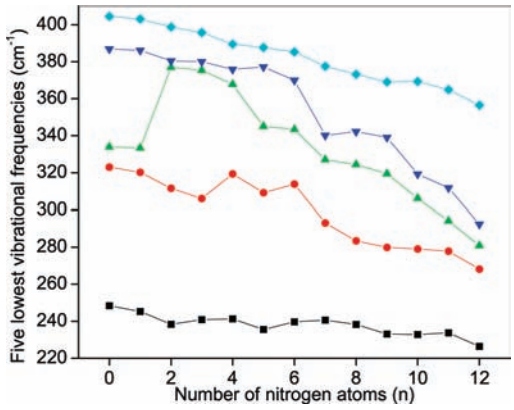

Figure 13. Variation of five lowest frequencies (cm^{-1}) as a function of the number of nitrogen atoms, $n = 0-12$.

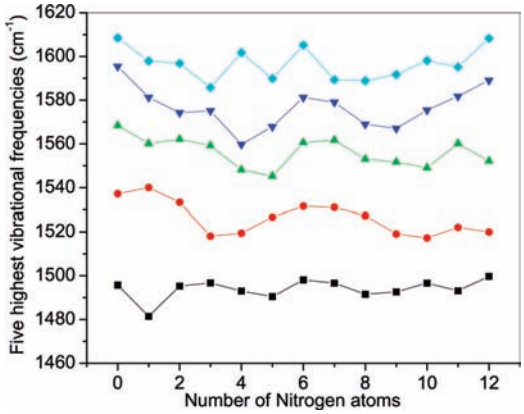

Figure 14. Variation of the highest frequencies (cm^{-1}) as a function of the number of nitrogen atoms, $n = 0-12$.

corrections have been included in the binding energy of all heterofullerene structures. However, the detailed results of vibrational frequencies will be presented separately.

IV. Conclusions

The detailed structural, electronic and, vibrational properties of nitrogen-doped fullerenes have been obtained by using linear density functional theory based ab initio calculations employing BLYP exchange interactions. From the structural analysis of all of the $C_{60-n}N_n$ heterofullerenes and their isomers, it is found that nitrogen atoms relax the fullerene structure and distribute themselves in such a way that not more than one nitrogen atom is substituted in the ring for $n = 1$, 3, 5, and 7. For $n = 2$, 4, 6, 8, 9, 10, 11, and 12, a combination of one and two nitrogen atoms in the hexagon rings is found to be more stable than other combinations considered. However, if we substitute four or more carbon atoms in the pentagon or hexagon rings with nitrogen atoms, the fullerene structure opens up by breaking the N−N bond. Each heterofullerene structure shows regioisomerism, showing a large number of structures with a very small difference in energy, and we have listed all of the possible regioisomers for $C_{58}N_2$ in Tables 3 and 4. The average C−C bond distance is found to be decrease from 1.46 to 1.43 Å, and the C=C bond distance is found to increase from 1.40 in C_{60} to 1.43 Å in $C_{48}N_{12}$. The C−N bond distance varies from 1.41 (6,5) and 1.43 Å (6,6) in $C_{59}N$ to 1.43 (6,5) and 1.45 Å (6,6) in $C_{48}N_{12}$. The structural deformation is found to increase with nitrogen doping.

The difference between the maximum and minimum diameter is found to increase gradually up to $n = 12$, except for $n = 3$ and 7, which show a small decrease in this difference. However, the average radius of $C_{60-n}N_n$ is found to be the same as that for C_{60} up to $n = 5$ and decreases thereafter to a minimum value of 7.06 Å. The change in the average diameter signifies the volume contraction, which is also a maximum for $C_{48}N_{12}$.

The electronic HOMO−LUMO gap of semiconducting C_{60} lowers by nitrogen substitution significantly from 1.67 for C_{60} to 0.55 eV for $C_{48}N_{12}$. However, no systematic pattern comes out as a function of nitrogen doping. The HOMO energy level shows a gradual increase, indicating a shift with doping. The effect of electronic polarization due to nitrogen is more pronounced at the NN carbon atoms around the nitrogen atom which shows charge gain from a nitrogen atom. Therefore, nitrogen behaves as an electron donor, and the first nearest carbon atoms exist as acceptors. The carbon atoms beyond 2NNs exist both as donors and charge acceptors, with a small net Mulliken charge on the order of ±0.004.

The harmonic vibrational frequencies for $C_{60-n}N_n$ are found to decrease as a function of nitrogen doping. The decrease in the frequency of different modes is found in the range of 15−79 cm^{-1}, which may be attributed to an increase in the molecular mass. The vibrational frequencies of doped heterofullerenes reported here motivates further experimental work to measure these. Nitrogen doping in fullerene molecules presents a interesting way to alter electronic and chemical properties of the C_{60} molecule for useful device applications.

Acknowledgment. The authors are thankful to the SIESTA group for providing their computational code. I.G. is thankful to the University Grant Commission for providing financial support.

References and Notes

(1) Dresselhaus, M. S.; Dresselhaus, G.; Eklund, P. C. *Science of fullerenes and carbon nanotubes*; Academic: NewYork, 1996.
(2) Guo, T.; Jin, C.; Smalley, R. E. *J. Phys. Chem.* **1991**, *95*, 4948.
(3) Hummelen, J. C.; et al. *Science* **1995**, *269*, 1554.
(4) Hultman, L.; Stafstrom, S.; Czigany, Z.; Neidhardt, J.; Hellegren, J.; Brunell, I. F.; Suenaga, K.; Colliex, C. *Phy. Rev. Lett.* **2001**, *87*, 225503.
(5) Liu, F. L. *Phys. Chem. Chem. Phys.* **2007**, *9*, 3872.
(6) Billas, I. M. L.; Tast, F.; Branz, W.; Malinowski, N.; Heinebrodt, M.; Martin, T. P.; Boeroa, M.; Massobriob, C.; Parrinello, M. *Eur. Phys. J.* **1999**, *D 9*, 337.
(7) Matsubara, M.; Massobrio, C. *Appl. Phys. A* **2007**, *86*, 289.
(8) Fu, C. C.; Weissmann, M.; Machado, M.; Ordejon, P. *Phys. Rev. B* **2001**, *63*, 085411.
(9) Xie, R. H.; Nalwa, H. S. *Advanced electronic and photonic materials and devices Nonlinear optical materials*; Academic Press: NewYork 2000; Vol. 9, Chapter 6, p 267.
(10) Monaa, M. R.; Xie, R. H.; Smith, V. H. J. *Chem. Phys. Lett.* **2004**, *387*, 101.
(11) Xie, R. H.; Bryant, G. W.; Zhao, J.; Smith, V. H., Jr.; di Carlo, A.; Pecchia, A. *Phys. Rev. Lett.* **2003**, *90*, 206602.
(12) Xie, R. H.; Bryant, G. W.; Sun, G.; Kar, T.; Chen, Z.; Smith, V. H., Jr.; Araki, Y.; Tagmatarchis, N.; Shinohra, H.; Ito, O. *Phys. Rev. B* **2004**, *69*, 201403(R).
(13) Lamparth, I.; Number, B.; Schick, G.; Skiebe, A.; Grosser, T.; Hirsch, A. *Angew. Chem., Int. Ed. Engl.* **1995**, *35*, 2257.
(14) Yu, R.; Zhan, M.; Cheng, D.; Yang, S.; Liu, Z.; Zheng, L. *J. Phys. Chem.* **1995**, *99*, 1818.
(15) Pradeep, T.; Vijayakrishnan, V.; Santra, A. K.; Rao, C. N. R. *J. Phys. Chem.* **1991**, *95*, 10564.
(16) Otero, V.; Biddau, G.; Sanchez, C. S.; Caillard, R.; Lopez, M. F.; Rogero, C.; Palomares, F. J.; Cabello, N.; Basanta, M. A.; Ortega, J.; Mendez, J.; Echavarren, A. M.; Perez, R.; Lor, B. G.; Gago, J. A. M. *Nature* **2008**, *454*, 865.
(17) Wang, S. H.; Chen, F.; Fann, Y. C.; Kashani, M.; Malaty, M.; Jansen, S. A. *J. Phys. Chem.* **1995**, *99*, 6801.
(18) Kurita, N.; Kobayashi, K.; Kumahora, H.; Tago, K. *Phys. Rev. B* **1993**, *48*, 4850.
(19) Chen, Z.; Zhao, X.; Tang, A. *J. Phys. Chem. A* **1999**, *103*, 10961.
(20) Chen, Q.; Li, J. *Chin. J. Struct. Chem.* **1997**, *16*, 445.

(21) Chen, Q.; Li, J.; Li, L.; Chen, H. *Chin. J. Struct. Chem.* **1998**, *17*, 417.
(22) Manaa, M. R. *Solid State Commun.* **2004**, *129*, 379.
(23) Qiang Hou, J.; Soek Kang, H. *J. Phys. Chem. A* **2006**, *110*, 12241.
(24) Bajwa, N.; Ingale, A.; Avasthi, D. K.; Ravi, K.; Tripathi, A.; Dharamvir, K.; Jindal, V. K. *J. Appl. Phys.* **2008**, *104*, 054306.
(25) Kaur, N.; Gupta, S.; Dharamvir, K.; Jindal, V. K. *Proceedings of the 26th International Symposium on Shock Waves ISSW26*; Springer-Verlag: Germany, 2007.
(26) Kaur, N.; Gupta, S.; Dharamvir, K.; Jindal, V. K. *Carbon* **2008**, *46*, 349.
(27) Kaur, N.; Dharamvir, K.; Jindal, V. K. *Chem. Phys.* **2008**, *344*, 176.
(28) Ordejon, P.; Artacho, E.; Soler, J. M. *Phys. Rev. B* **1996**, *53*, R10441.
(29) Soler, J. M.; Artacho, E.; Gale, J. D.; Garca, A.; Junquera, J.; Ordejn, P.; Portal, D. S. *J. Phys.: Condens. Matter* **2002**, *14*, 2745.
(30) Junquera, J.; Paz, O.; Sanchez-Portal, D.; Artacho, E. *Phys. Rev. B* **2001**, *64*, 235111.
(31) Becke, A. D. *Phys. Rev. A* **1998**, *38*, 3098.
(32) Lee, C.; Yang, W.; Parr, R. G. *Phys. Rev. B* **1988**, *37*, 785.
(33) Miehlich, S.; Stoll, P. *Chem. Phys. Lett.* **1989**, *157*, 200.
(34) Kleinman, L.; Bylander, D. M. *Phys. Rev. Lett.* **1982**, *48*, 1425.
(35) Sankey, O. F.; Niklewski, D. J. *Phys. Rev. B* **1989**, *40*, 3979.
(36) Hertel, I. V.; Steger, H.; de Vries, J.; Weisser, B.; Menzel, C.; Kamke, B.; Kamke, W. *Phys. Rev. Lett.* **1992**, *68*, 784.
(37) Wang, X. C.; Ding, C. F.; Wang, L. S. *J. Chem. Phys.* **1999**, *110*, 8217.
(38) Rivelino, R.; de Brito Mota, F. *Nano Lett.* **2007**, *7*, 1526.
(39) Wang, K. A.; Rao, A. M.; Eklund, P. C.; Dresselhaus, M. S.; Dresselhaus, G. *Phys. Rev. B* **1993**, *48*, 11375.
(40) Dong, Z. H.; Zhou, P.; Holden, J. M.; Eklund, P. C.; Dresselhaus, M. S.; Dresselhaus, G. *Phys. Rev. B* **1993**, *48*, 2862.
(41) Xie, R. H.; Bryant, G. W.; Jensen, L.; Zhao, J.; Smith, V. H., Jr. *J. Chem. Phys.* **2003**, *118*, 8621.

JP901969Z